

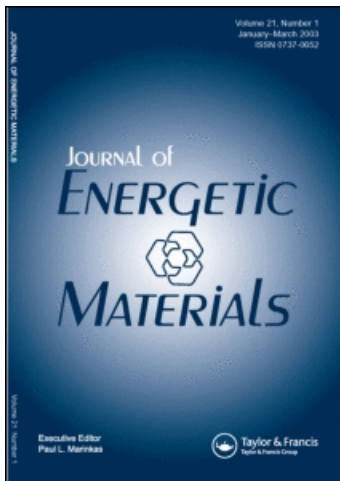
This article was downloaded by:

On: 16 January 2011

Access details: *Access Details: Free Access*

Publisher *Taylor & Francis*

Informa Ltd Registered in England and Wales Registered Number: 1072954 Registered office: Mortimer House, 37-41 Mortimer Street, London W1T 3JH, UK



## Journal of Energetic Materials

Publication details, including instructions for authors and subscription information:

<http://www.informaworld.com/smpp/title~content=t713770432>

### Recrystallization of CL-20 and HNFx from Solution for Rigorous Control of the Polymorph Type: Part I, Mathematical Modeling using Molecular Dynamics Method

Z. Peralta-Inga<sup>a</sup>; N. Degirmenbasi<sup>a</sup>; U. Olgun<sup>a</sup>; H. Gocmez<sup>a</sup>; D. M. Kalyon<sup>a</sup>

<sup>a</sup> Stevens Institute of Technology, Castle Point Station, Hoboken, NJ

**To cite this Article** Peralta-Inga, Z. , Degirmenbasi, N. , Olgun, U. , Gocmez, H. and Kalyon, D. M.(2006) 'Recrystallization of CL-20 and HNFx from Solution for Rigorous Control of the Polymorph Type: Part I, Mathematical Modeling using Molecular Dynamics Method', *Journal of Energetic Materials*, 24: 2, 69 – 101

**To link to this Article:** DOI: 10.1080/07370650600672082

**URL:** <http://dx.doi.org/10.1080/07370650600672082>

PLEASE SCROLL DOWN FOR ARTICLE

Full terms and conditions of use: <http://www.informaworld.com/terms-and-conditions-of-access.pdf>

This article may be used for research, teaching and private study purposes. Any substantial or systematic reproduction, re-distribution, re-selling, loan or sub-licensing, systematic supply or distribution in any form to anyone is expressly forbidden.

The publisher does not give any warranty express or implied or make any representation that the contents will be complete or accurate or up to date. The accuracy of any instructions, formulae and drug doses should be independently verified with primary sources. The publisher shall not be liable for any loss, actions, claims, proceedings, demand or costs or damages whatsoever or howsoever caused arising directly or indirectly in connection with or arising out of the use of this material.

## Recrystallization of CL-20 and HNFx from Solution for Rigorous Control of the Polymorph Type: Part I, Mathematical Modeling using Molecular Dynamics Method

Z. PERALTA-INGA  
N. DEGIRMENBASI  
U. OLGUN  
H. GOCMEZ  
D. M. KALYON\*

Stevens Institute of Technology, Castle Point Station,  
Hoboken, NJ

*The recrystallization of CL-20 and HNFx to form different polymorphs was investigated by employing combinations of computations (polymorph predictions with and without the presence of the solvent molecules in the molecular dynamics based calculations) and experimental analyses, including micro-crystallization under a myriad of conditions, novel means of crystallization, analysis of polymorphs using X-ray powder diffraction, and Rietveld analysis, and the use of conventional methods including DSC, TGA, polarized microscopy and SEM (with the experimental results reported in Part II of this paper). In the investigation all three groups of solvents: polar protic, non-polar aprotic, and dipolar aprotic solvents were employed. Our computations have revealed (in agreement with earlier studies) that polymorphs with various densities for both CL-20 and HNFx are possible. However, as part II of this paper will show although the experiments revealed different polymorph types,  $\alpha$ ,  $\beta$ ,  $\gamma$ ,  $\epsilon$  for CL-20 under different recrystallization conditions all of our*

\*Address correspondence to [dkalyon@stevens.edu](mailto:dkalyon@stevens.edu)

*experimental work for HNFx have resulted in crystals pertaining to Ci R-3, which is the only known polymorph of HNFx.*

**Keywords:** Ci R-3, CL-20, DSC, HNFx, micro-crystallization, polymorph predictions, Rietveld analysis, SEM, TGA

## Introduction

The use of difluoramines as energetic materials has been pursued for decades, especially for systems containing Al and B [1,2]. The difluoroamine group provides significant energy upon decomposition, but its presence also renders the molecule very sensitive to shock and relatively thermally unstable [1]. Two different approaches have been employed for the synthesis of energetic difluoramines, including -difluoramination of heterocyclics [3] and dinitromethyl anions [4] with  $\text{NF}_2\text{OSO}_2\text{F}$  and the formation of geminal difluoroamino groups by reacting ketones with difluoroamine in fuming sulfuric acid [1]. One of the most interesting energetic materials containing the difluoroamine group synthesized recently is 3,3,7,7-tetrakis (difluoroamino) octahydro-1, 5-dinitro-1, 5-diazocine (HNFx) [5] HNFx was synthesized by the nitration of 3,3,7,7-tetrakis (difluoroamino) octahydro-1, 5-bis (4-nitrobenzenesulfonyl)-1,5-diazocine with  $\text{HNO}_3/\text{CF}_3\text{SO}_3\text{H}$  at  $55^\circ\text{C}$  for 40 h [1].

The performance characteristics of energetic formulations, including the detonation velocity and pressure during combustion are directly linked to the density of the energetic crystals [6]. The stumbling block to the development of various nitramines as suitable materials for use in energetic formulations is the difficulty of generating specific gravity values that approach 2.0. Under this constraint, HNFx (Fig. 1) was considered a suitable energetic material principally as a result of computations that indicated that the density of HNFx could be as high as 1.945 g/cc [Ammon, U. Md. calculations, information from ONR]. However, upon the crystallization of HNFx and the subsequent analysis of its crystalline structure and density

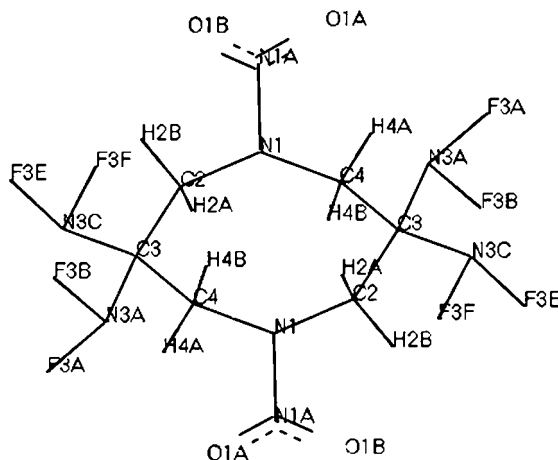


**Figure 1.** HNFx molecular structure.

using X-ray crystallography, it was determined that the density of the currently available HNFx is only 1.807 g/cc. This low density value is considered to be the result of the specific crystal packing in which three molecules form the surface of a cylinder with an empty core believed to be due to solvent interactions: as stated by Chapman et al.:

“... presence of disordered mass due to recrystallization solvents. Though solvent free crystals can be readily prepared by driving out the solvents by heating or vacuum all crystals analyzed so far have retained these channels. The crystal density of the form produced so far is 1.807 g/cm<sup>3</sup> if a vacuum is assumed in the channels” [5].

Chapman et al. have also tried to synthesize HNFx through a second synthesis route which eliminates the use of solvents, however, this route leads to nosyl derivatives of HNFx [5]. The crystalline samples of the result of this second route have been analyzed with X-ray analysis also and have indicated that higher densities can be obtained (up to 1.863 g/cc).

Ammon’s calculations and predictions show that the HNFx experimental crystal structure in space group R-3 is not the lowest energy at  $-39.7 \text{ kcal mol}^{-1}$ . They predicted a

(presently) unknown polymorph in space group P21/c with a substantially lower energy of about  $-44 \text{ kcal mol}^{-1}$  and higher density of about  $2.03 \text{ g/cm}^3$  [7]. Chapman et al. [5] noted that more dense polymorphs may be found in the future, in a manner similar to both CL-20 and HMX, which had only low-density polymorphs isolated initially. Our investigation has aimed at recrystallizing HNFx using myriad techniques, computational as well as experimental, to arrive at significantly denser polymorphs.

The second material of our study, CL-20 was developed as a crystalline explosive at the Naval Weapons Center at China Lake in 1989. Several polymorphs of CL-20 crystal are known to exist. Currently the epsilon phase is the one that is targeted and under extensive investigation. It provides high density, lower sensitivity, and high-energy output upon detonation. The polymorphic purity is one of the primary measures of end-product quality and is becoming increasingly important in the specialty chemical as well as in the explosive industries. Therefore, one of the key steps is the identification of the right solvent or solvent mixtures that can selectively produce the desirable crystalline phase. In general, the epsilon CL-20 is highly soluble in the solvents with carbonyl groups, and is relatively insoluble in hydrocarbons and materials containing ether linkages [8].

Bulk density, mechanical strength, sensitivity, storage, and handling can be very different for each polymorph. Selective preparation of the desirable polymorph is possible by solution crystallization. Specific crystal shape and size distribution can also be achieved by controlling the crystal growth conditions. The phase behavior that controls purity, and the kinetics that defines size distribution, are critical in the design of organic solids. Selection of proper solvent/anti-solvents and their mixtures is the most difficult step in controlling the phase behavior. The objective of the investigation was to mathematically model the crystallization process to predict the polymorph to be generated and then validate the polymorph type using X-ray diffraction, XRD, in conjunction with Rietveld analysis.

## Objectives

The objectives of our research were the following:

1. Develop mathematical modeling and experimental means for crystallization of HNFx and CL-20. This includes setting up computational procedures to predict polymorph type in the absence and presence of solvents, setting up a recrystallization facility for HNFx and CL-20 for experimental validation of the simulation results, setting up powder diffraction and Rietveld techniques for the determination of the polymorph types, and setting up other conventional characterization means for the analysis of the pertinent properties of CL-20 and HNFx, including TGA, DSC, polarized microscopy, SEM etc.
2. Investigate the crystallization of CL-20 and HNFx using a combination of theoretical and experimental means, systematically starting with simple approaches to recrystallization, involving a single or combination of solvents (solvents/anti-solvents), and other novel means including the use of gel crystallization, and microwaves etc.
3. As a general approach, the simulation results were used to determine suitable conditions and materials for crystallization to give rise to the desired polymorphs of CL-20 and HNFx, which should exhibit higher densities than currently available. Experimental means were then applied to validate the predictions of the computations. Priority was given to low cost and environmentally friendly solvent systems.

## Methods

### *Computational Modeling and Simulation*

Polymorph prediction by using computational tools has been popular after the recent development in computational chemistry that allows the prediction of possible polymorph forms based on the molecular structure of the materials [9]. Basically,

a polymorph predictor would generate all of the possible crystal forms of a molecule, rank them in terms of lattice energy, and offer a measure for which structures are most likely to form under various condition of crystallization [10]. There are a few different approaches that can predict the possible polymorph of an organic compound from its molecular structure. A typical procedure is the following:

- A Monte Carlo simulated annealing process searches the lattice energy hyper-surface for probable crystal packing alternatives, typically generating thousands of possible structures
- These potential structures are clustered into unique groups based on packing similarity
- Each unique structure is minimized with respect to all degrees of freedom
- The minimized structures are clustered again to remove duplicates
- The final structures are ranked according to lattice energy

The resulting low energy crystal structures are potential polymorphs. Theoretically, there are many limitations in using polymorph prediction methods. First, the *ab initio* screening is only useful for nonionic rigid molecules. Second, computer power is generally not sufficient to process the polymorph prediction of large and complex molecules. The existing methods consider only lattice energy during the polymorph prediction. However, the relative thermodynamic stability of polymorphs is determined by Gibbs free energy, which is a linear function of both enthalpy and entropy [9]. As a result, although present methods and software may be useful in providing a set of structures as possible polymorphs for a given molecular structure, there is no accepted procedure available yet for polymorph prediction [11,12]. It should be noted that the conventional techniques of polymorph prediction are carried out in vacuum conditions—thus, they diverge from actual crystallization conditions including solvents etc.

Let us first see what is available in the literature in the area of prediction of the polymorphs of various energetic molecules without considering the effect of the solvents and thus under vacuum. Generally one determines the smallest lattice energy of the molecule predicted for various different structures. The minimum lattice energy is considered to predict the correct structure. A compilation by Ammon et al. [7] indicates that the use of molecular modeling under vacuum conditions has previously successfully predicted the correct structures of various energetic crystals including RDX and epsilon CL-20. Yet, it was not able to predict the correct structures of other energetic crystals such as beta HMX.

The comparisons of various techniques of crystal structure predictions were carried out in a double-blind studies at the Cambridge Crystallographic Data Center to test how well currently available computational methods of crystal structure prediction perform when only the atomic connectivity for an organic compound is provided [11,12]. In both studies few participants, using different methods, could predict structures that were close to the experimental ones to be classified as correct. However, it was determined that many structures were found to differ only within a few kcal/mol of each other (around the global minimum) and thus no method tested in this 2000 and 2002 studies could generate consistently correct results [11,12]. This suggests that the details of the procedures used, for example the force field, which is utilized, and the method of parameterization influence the energy ranking of the predicted structures, giving rise to rather different results in some cases.

Understanding the successes and the current limitations of the computational methods for polymorph prediction and in the attempt to search for both the energetically feasible structures and the kinetically favored structures in our study, we have applied two computational strategies:

1. Polymorph prediction in the absence of solvents
2. Polymorph prediction in presence of solvents

*Polymorph Prediction in the Absence of Solvents.* In the first part of our investigation we aimed to compare our

methodologies with the results available in the literature for the under vacuum computations of structure prediction for HNFx. Our approaches for the structure prediction of HNFx and polymorph prediction under vacuum conditions are described below and utilized the Cerius 2 software and its various modules.

The crystal structure of HNFx reported by Chapman et al. was obtained from CCDC resource and accessed using Encifer software. From this, the atomic structure of HNFx (Fig. 1) was extracted and the unit cell of HNFx (Fig. 2) was built using C2 crystal builder. After minimization, of the atomic structure, crystal structure predictions were carried out using Polymorph Predictor [14]. The procedure included the following steps:

1. HNFx molecule was loaded.
2. An appropriate force field was selected. Molecular mechanisms have been completely dependent on the

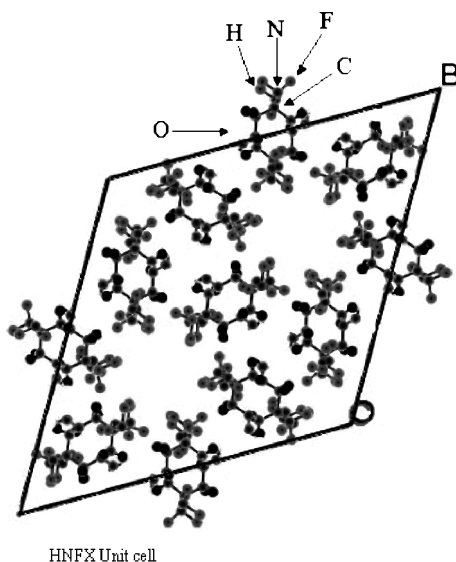


**Figure 2.** HNFx unit cell built with Cerius<sup>2</sup> [13] crystal builder.

force field that is used to describe interactions between the atoms in the molecule. The force-field contains values for the force constants of the bond stretching, bond angle, bending, molecular bond torsion, and planar inversion energies as well as numerical convergence and cut off criteria for the non-bonded energy terms and the minimization algorithms [15,16]. We have worked with generally two force-fields, i.e., DREIDING 2.21 and COMPASS. However, most of our calculations were carried out with DREIDING 2.21. In DREIDING the form of the force field is defined on the basis of the potential energy for an arbitrary geometry of a molecule which is given as a superposition of the valence (or bonded) interactions that depend on the “specific connections (bonds) of the structure and the non-bonded interactions that depend on the distances between atoms” [17]. The valence interactions are made up of the bond stretch, bond angle bend, dihedral angle torsion, and the inversion terms [17] and the nonbonded interactions consist of van der Waals or dispersion, electrostatic, and explicit hydrogen bonds.

3. In some procedures we also used the COMPASS (Condensed Phase Optimized Molecular Potentials for Atomistic Simulation Studies) force field. COMPASS is an ab initio force field that enables simultaneous prediction of structural, conformational, vibrational, and thermophysical properties for a broad range of molecules in isolation and in condensed phases [18].
4. The Ewald long-range summation method for electrostatic interactions was selected using an open force field. This method exploits the periodicity of the system by calculating part of the summations in reciprocal space. The Ewald method converges energy faster and a more accurate result can be obtained [19]. Atom charges, and ESP (electrostatic potential derived) charges were calculated with MOPAC6 (MOPAC is a general-purpose semi-empirical molecular orbital

package for the study of chemical structures and reactions. The semi-empirical Hamiltonians MNDO, MINDO/3, AM1, and PM3 are used in the electronic part of the calculation to obtain molecular orbitals, the heat of formation and its derivative with respect to molecular geometry were carried out to obtain charges in the molecule.

5. Rigid body constraints for the molecule were specified in the asymmetric unit in order to hold the molecule rigid during the minimization step of the polymorph prediction sequence.
6. In conjunction with the POLYMORPH PREDICTOR module of C2 first the number of molecules in the asymmetric unit was first specified before running the polymorph prediction module of C2. For instance, the number of molecules in the asymmetric unit for HNFx is 0.5, which means that only 17 atoms are enough to determine molecular structure of the crystal although the chemical formula of the HNFx contains 34 atoms. Unfortunately, the C2 polymorph module was designed for the molecules that have 1 or more molecules in the asymmetric unit. This is a weak point of the program.
7. The polymorph prediction module includes three sequences: Monte Carlo simulation, cluster analysis, and energy minimization. The first part of a polymorph prediction sequence is a Monte Carlo simulation of the thermodynamic movement of the system for each selected space group. The simulation consists of two phases, heating and cooling, and is also called *simulated annealing*. The Metropolis algorithm is used to determine whether the generated trial structures are accepted or rejected. In the C2, the Monte Carlo method is used in conjunction with constraints in search parameters and space groups to reduce the simulation time, otherwise polymorph prediction incorporates scans of all possible space groups during the simulation.

8. The second part of the polymorph prediction includes cluster analysis that determines the structures having lowest energy disregarding the rest. Preference of the cluster analysis can be changed according to search level and parameters.
9. The last part of the polymorph prediction is energy minimization, which minimizes and optimizes the structures with respect to all degrees of freedom. Preference of the energy minimization can be changed according to the number of minimization steps and rigid bodies.
10. The polymorph prediction sequence thus included a Monte Carlo simulation and subsequent cluster analysis, minimization, and final clustering for each specified space group. The polymorphs generated during the run were saved in the trajectory files to analyze the properties of structures for further study.
11. Polymorph selection was completed by analysis of the predicted structures based on the density and lattice energy.

*Prediction of the Most Likely Polymorph in the Presence of Solvents.* There is currently no conventional model that can rigorously predict the type of polymorph for a given solvent system. However, the MD simulations of liquid phase and the solid-liquid interface are theoretically possible, and have been demonstrated for various materials [19]. MD methods have also been used to simulate the nucleation and crystallization of polymers [20]. Conformational changes in the polymer chain could be monitored in the presence of various nucleating agents.

Similar techniques were applied in our investigation to simulate the crystallization process of HNFx with different solvents. Our objective was to select appropriate solvents for HNFx crystallization and to determine the solvent that is most likely to generate a particular polymorph. Molecular Dynamic (MD) simulation techniques were used and the possible conformational changes and solvent-solute interactions occurring

during the crystallization process were monitored. After MD simulation, the energy calculation for each solvent-solute system was also carried out. From the interactions and differences in energy for each solute-solvent system, the solvents, and the antisolvents to be used in crystallization were selected. The most likely polymorph to be grown in a given solvent was predicted by performing the same type of MD calculations (solute-solvent system) where the solute is an HNFX or CL-20 polymorph previously predicted with the C2 polymorph predictor and the solvent is one of the solvents screened. The process was repeated for each solvent tested. Both non-periodic and periodic conditions were considered. The procedures followed are described below.

*Non-periodic conditions* This refers to the simulation of models consisting of an amorphous cell, which does not replicate in 3-D. MD simulations of HNFX with seven solvents in an amorphous cell were carried out. Overall, the procedure that is used for the non-periodic MD simulation includes the following steps:

1. An HNFX molecule (1) and proper amount of solvent molecules (32) were loaded under the non-periodic structure option.
2. An appropriate force field was selected. We have worked with generally two force fields, i.e., DREIDING 2.21, and COMPASS (mostly with DREIDING 2.21). In DREIDING the valance interactions are made up of the bond stretch, bond angle bend, dihedral angle torsion and the inversion terms [17]. The Ewald long-range summation method for electrostatic interactions was selected using open force field.
3. Charges were calculated with the charge equilibration (Qeq) method based on electronegativity and geometry. The charge equilibrium option was selected.
4. Energy was minimized by “Smart Minimizer” (~10000 iterations). Energy minimizations were carried out to find optimal arrangements of molecules in the unit cell.

5. Dynamics simulation NVT (MD, Constant-volume/constant-temperature dynamics) was initially selected at 300 K and in conjunction with 5000 steps. The NVT dynamics was modified to allow the system to exchange heat with the environment at a controlled temperature.
6. NVE (Constant-volume/constant-energy dynamics) was applied after NVT to bring up the system to an equilibrium state.

Final structures were minimized to calculate the energy of the model in its current conformation without changing atom positions at zero temperature Kelvin.

*Periodic boundary conditions (PBC).* Periodic boundary conditions refer to the simulation consisting of a periodic lattice of identical subunits. The molecules included in the simulation were kept within a cubic box, which replicated in all three directions (x, y, z). By applying periodic conditions to simulations, the influence, for example of bulk solvent of the crystalline environment could be included, thereby improving the rigor and realism of the model.

Periodic boundary conditions MD simulations were used, the simulations were performed in a solute-solvent system, in a 3D unit (simulation box) in which the solute was HNFx, or an HNFx predicted polymorph, and the solvents were varied. A group of twenty-three solvents corresponding to the three main categories of solvents classification were analyzed in each case. The simulation box was generated using the “C<sup>2</sup> Amorphous Builder.” The model involved further minimization and the simulations were carried out using NVT and NVE methods, for 10 ps. In the same fashion the MD simulation box was created for 32 molecules of each solvent. A molecule of HNFx from one of the predicted polymorphs was included in the solvent. NVT, NVE simulation was applied for 5000 steps, and the energy of the system was minimized. The same procedure was repeated for all the predicted polymorphs obtained in the polymorph prediction trail. Overall the

procedure for MD simulation with periodic boundary condition included the following steps:

1. HNFx molecule (1) and proper amount of solvent molecules (32) were loaded by using Amorphous Builder in conjunction with the 3D periodic structure.
2. An appropriate force field was selected. Our calculations were carried out with DREIDING 2.21. In DREIDING the valence interactions are made up of the bond stretch, bond angle bend, dihedral angle torsion and the inversion terms [17]. The Ewald long-range summation method for electrostatic interactions was selected using open force field.
3. Charges were calculated with the charge equilibration (Qeq) method based on electronegativity and geometry. The charge equilibrium option was employed.
4. Energy was minimized by the use of the Smart Minimizer routine ( $\sim 10000$  iterations). Energy minimizations were carried out to find optimal arrangements of molecules in the unit cell.
5. Dynamics simulation NVT (Constant-volume/constant-temperature dynamics) was initially selected at 300 K with 5000 steps. The NVT dynamics was modified to allow the system to exchange heat with the environment at a controlled temperature.
6. NVE (Constant-volume/constant-energy dynamics) was applied for 5000 steps after NVT to bring up the system in equilibrium state.
7. Final structures were minimized to calculate the energy of the model in its current conformation without changing atom positions at zero temperature K.

## Results

### *Computational Modeling and Simulation*

The crystal structure of HNFx (reported by Chapman et al. [5]) was obtained from the CCDC resource, accessed using Encifer software, and visualized with C2 visualizer. From this, the atomic structure of HNFx presented in Fig. 1 was obtained.

The atoms, F3A-N3A-F3B, F3E-N3C-F3F, F3G-N3D-F3H, F3C-N3B-F3D, are occupied 0.9, 0.66, 0.34, and 0.1 (suggesting sharing between various neighboring unit cells), respectively in the HNFx molecule. The unit cell of HNFx was built using C2 crystal builder, and is shown in Fig. 2.

*Polymorph Prediction in the Absence of Solvents for HNFx.*

The starting structure was the HNFx molecule presented in Fig. 1. The structure was minimized. After minimization, the Polymorph procedure described in the methodology section was applied. The results of our polymorph predictions in absence of solvents (under vacuum) are shown in Table 1. C2 polymorph predicted the most favorable 4 different space groups of HNFx. These are Pca2<sub>1</sub>, P2<sub>1</sub>/c, Cc, P2<sub>1</sub>2<sub>1</sub>2<sub>1</sub>. Their predicted lattice energy values are -37.6, -42.08, -43.51, and -42.99 kcal/mol respectively. The density of the predicted polymorphs varies between 1.843 and 1.892 g/cm<sup>3</sup> when the Dreiding 2.21 force field is used. In addition, COMPASS (condensed phase optimized molecular potentials for atomistic simulation studies) force field was used to optimize final structures and also provide better packing density, which varies between 2.057 and 2.123 g/cm<sup>3</sup>. These results are also included in Table 1.

**Table 1**

Polymorph prediction in the absence of solvents (in vacuum)

Model geometry	Crystal symmetry	Space group	Lattice E (kcal/mol)	Density* (g/cm <sup>3</sup> )	Density** (g/cm <sup>3</sup> )
C <sub>i</sub> , model	Orthorhombic	Pca2 <sub>1</sub>	-37.6	1.874	2.108
C <sub>i</sub> , model	Monoclinic	P2 <sub>1</sub> /c	-42.08	1.892	2.117
C <sub>i</sub> , model	Monoclinic	Cc	-43.51	1.843	2.057
C <sub>i</sub> , model	Orthorhombic	P2 <sub>1</sub> 2 <sub>1</sub> 2 <sub>1</sub>	-42.99	1.858	2.078
C <sub>1</sub> , model	Monoclinic	P2 <sub>1</sub> /c	-42.50	1.869	2.123

\*Dreiding force Field was used.

\*\*Compass force Field was used to optimize structure given by C2 polymorph prediction module.

Table 2 shows the lattice energies for various polymorphs predicted and compared with the literature values (Ammon's prediction). From this table we can see that the lattice energy values and densities predicted and are quite similar to those in the literature. The slight differences should be primarily due to the use of different geometry optimization routines during the polymorph prediction. Ammon et al. [7] used Gaussian 94 for geometry optimization and partial charge calculation, whereas we used MOPAC6 for the same purpose.

A second polymorph prediction under vacuum was performed. This time, the DREIDING 2.21 force field and COMPASS force field were used consecutively. The results are presented in Table 3. These results indicate that the crystal structures obtained have a lower lattice energy and higher density than crystal structures predicted with DREIDING as shown earlier in Table 1.

Figure 3 shows the angular conformation of the HNFx molecule in an R-3 polymorph (the low-density polymorph of the as-received HNFx samples from China Lake). Figs. 4–7 show the conformational changes of an HNFx molecule in other predicted polymorphs to be compared with the R-3 polymorph. The conformations of the HNFx molecules in each polymorph are different on the basis of the conformation of the N–F bonds, which are open outwards or inwards from the plane of symmetry to different degrees in different space groups. Measurements for the angles that involved N-F bonds (F-N-F angles) for the R-3 Polymorph (as received HNFx) and the possible other polymorphs, predicted to occur likely, are included in each figure.

### *Polymorph Prediction in the Presence of Solvents*

*Non-periodic conditions.* As it was described in the methodology section, non-periodic conditions refers to the simulation in an amorphous cell, a model, in which the solute is surrounded by solvent molecules without a boundary and does not replicate in 3D directions. Figure 8 shows the typical case of one molecule of HNFx surrounded by 10 molecules of acetone solvent in amorphous form. MD simulations of HNFx with seven different solvents under non-periodic conditions were

**Table 2**  
Computations for the most-likely polymorphs of HNFx at SIT

Model geometry	Crystal symmetry	Space group	Lattice E (kcal/mol) (predicted at SIT)	Density* (g/cm <sup>3</sup> ) (predicted at SIT)	Density** (g/cm <sup>3</sup> ) (predicted at SIT)	Lattice E (kcal/mol) (predicted at Ammon)	Density (g/cm <sup>3</sup> ) (predicted at Ammon)
C <sub>i</sub> , model	Orthorhombic	Pca2 <sub>1</sub>	-37.6	1.874	2.108	-41.19	1.945
C <sub>i</sub> , model	Monoclinic	P 2 <sub>1</sub> /c	-42.08	1.892	2.117	-43.39	2.049
C <sub>i</sub> , model	Monoclinic	Cc	-43.51	1.843	2.057	-39.38	1.944
C <sub>i</sub> , model	Orthorhombic	P2 <sub>1</sub> 2 <sub>1</sub> 2 <sub>1</sub>	-42.99	1.858	2.078	-41.03	1.963
C <sub>1</sub> , model	Monoclinic	P 2 <sub>1</sub> /c	-42.50	1.869	2.123	-37.72	1.917

\*Dreiding force field was used.

\*\*Compass force field was used to optimize structure given by C2 polymorph prediction module.

**Table 3**  
Polymorph prediction in the absence of solvents using  
COMPASS

Crystal symmetry	Space group	Lattice E (kcal/mol)	Density (g/cm <sup>3</sup> )
Orthorhombic	Pca2 <sub>1</sub>	-138.00	2.19
Monoclinic	P2 <sub>1</sub> /c	-139.50	2.21
Orthorhombic	P2 <sub>1</sub> 2 <sub>1</sub> 2 <sub>1</sub>	-139.31	2.228
Monoclinic	P2 <sub>1</sub>	-140.35	2.254
Monoclinic	C 2/c	-139.98	2.129

carried out. Thirty-two molecules of each solvent (i.e., acetone, chloroform, acetophenone, cyclohexanone, dichloromethane, ethanol, and ethyl acetate) were used with HNFx or each predicted polymorph of HNFx. Energy calculations were carried out after each non-periodic MD run to allow the better

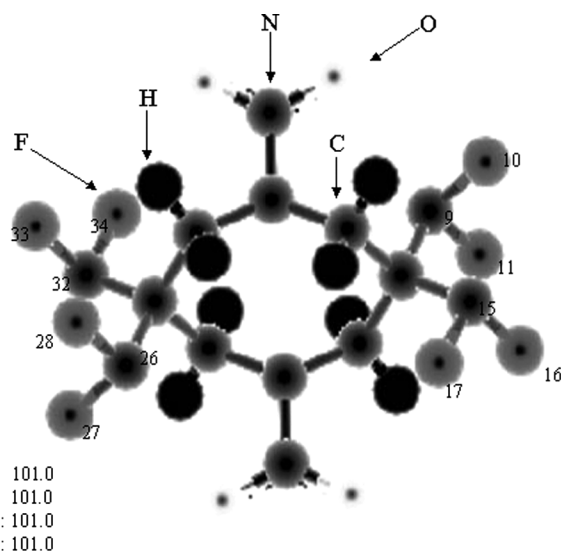


**Figure 3.** Angular conformation of the HNFx molecule in the R-3 polymorph (experimental).

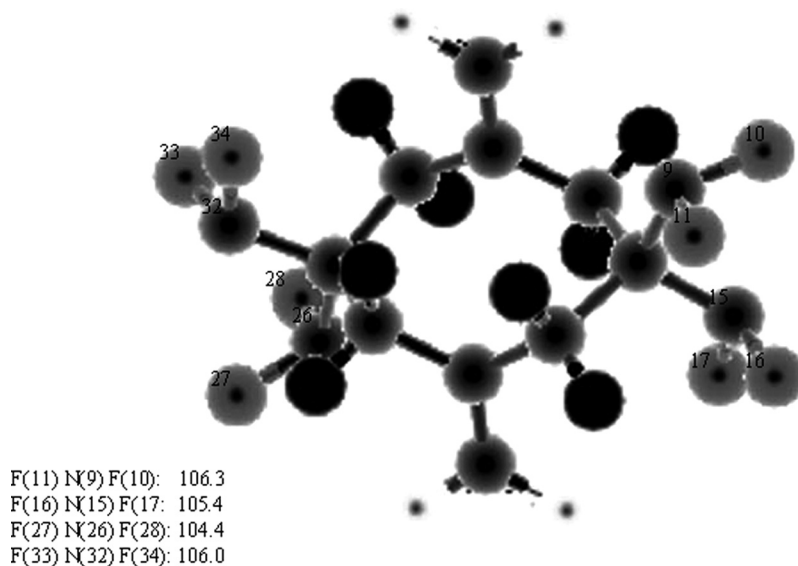


**Figure 4.** Angular conformation of the HNFx molecule in the  $Pca2_1$  polymorph.

relaxation of the system. The simulation results obtained for HNFx with these seven solvents under non-periodic conditions are presented in Table 4.

The first column of Table 4 shows the minimized energy of the HNFx (R-3) molecule with seven solvents after molecular dynamics simulation. The relative stability of polymorphs can be determined by the values of the Gibbs free energy change ( $\Delta G$ ) at a given temperature and pressure.

$$\Delta G = \Delta H - T\Delta S$$

where  $\Delta H$  is the enthalpy change of the system,  $T$  is the temperature and  $\Delta S$  is the entropy change of the system. A negative  $\Delta G$  indicates that the process to generate a given polymorph is likely to occur spontaneously. It is known that entropy term is always positive, which means that  $\Delta H$  is indeed the determining factor for the stability of the polymorph [14].

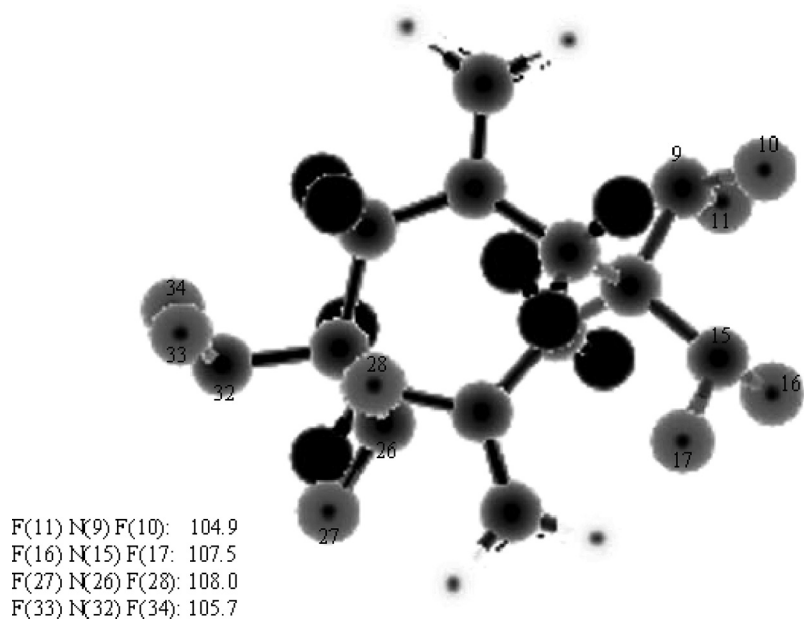


**Figure 5.** Angular conformation of the HNFx molecule in the P<sub>21c</sub> polymorph.

When different pairings of the solvent and polymorphs are simulated to determine their energy configurations, the lower energy states suggest a greater probability for the formation of stable polymorphs. For example, if the solvent ethyl acetate is considered the calculated energy for the ethyl acetate and HNFx R-3 (the space group of the as-received crystals of HNFx) pair gives rise to the lowest energy state in comparison to other polymorphs. This suggests that when ethyl acetate is used as the solvent, the most likely polymorph is indeed the currently prevailing polymorph of HNFx, which is experimentally validated. The same is true, when acetophenone is used. Table 4 also suggests that the predicted energy for the R-3 is very close to the lowest energy state for the other five solvents. In some cases however, one of the other polymorphs gives rise to a lower energy state, indicating that there is a probability for the formation of other polymorphs when solvents other than ethyl acetate

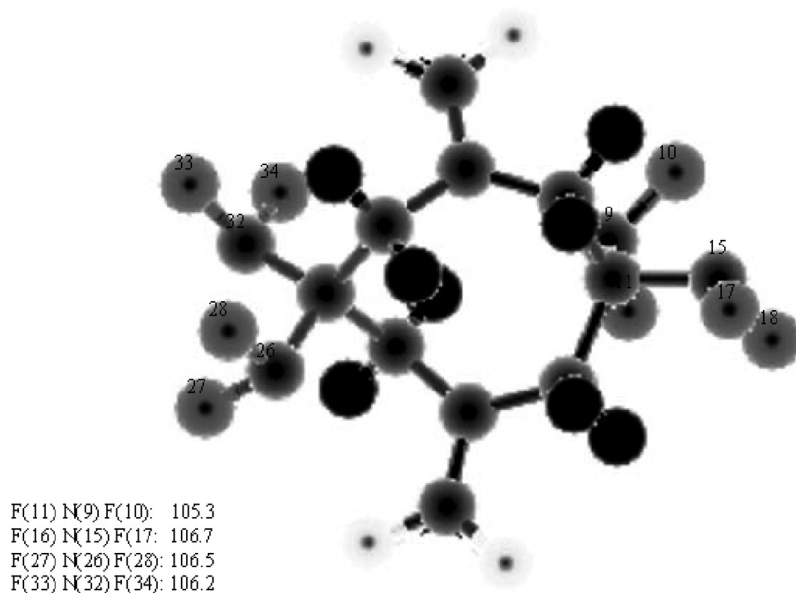


**Figure 6.** Angular conformation of the HNFx molecule in the Cc polymorph.

and acetophenone are used. Overall, these results obtained for the non-periodic condition suggest that in general the R-3 polymorph (as-received polymorph of HNFx) is predicted to be the dominant form, but other polymorphs are predicted to be possible with various other solvents, with R-3 representing a high probability, however, for all solvents. As will be shown in Part II of this paper however, experimental studies revealed that R-3 was indeed the only polymorphs generated when any of these solvents were used.

*Periodic conditions.* The MD simulations were also performed using a second approach, i.e., with the periodic boundary conditions as described earlier, for different pairs of solute-solvent systems, by employing a 3D simulation box (that replicates in all three directions). Twenty-three different

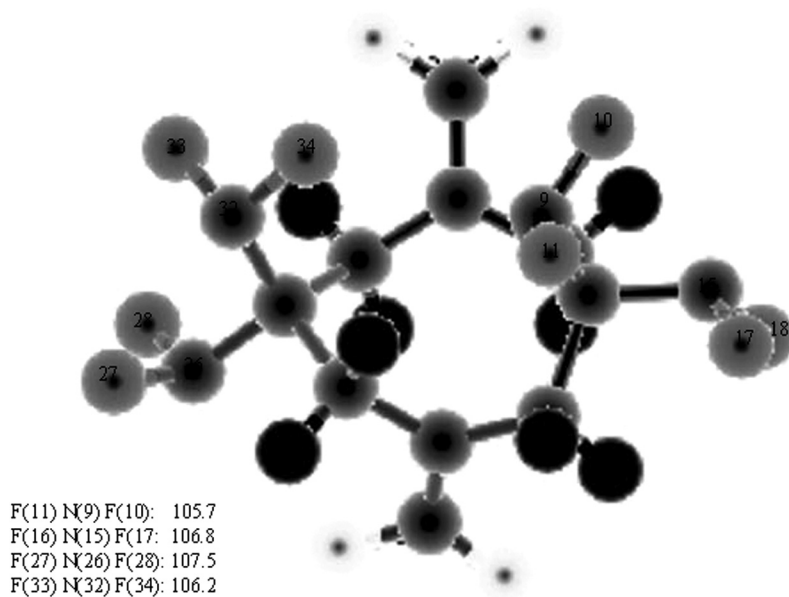


**Figure 7.** Angular conformation of the HNFx molecule in the  $P2_12_12_1$ .

solvents that included three classes of solvents: polar, dipolar aprotic, and non-polar aprotic solvents were analyzed in conjunction with the periodic condition. For example, Fig. 9 shows the typical case of one molecule of HNFx surrounded by 10 molecules of ethyl acetate (ETAC, with a density of 0.89 g/cc) solvent in the 3D unit (simulation box).

The results of these simulations are shown in three tables arranged by the type of solvent based on the nature of their molecular bonding interactions. Table 5 shows the results for polar solvents. Table 6, shows the results for dipolar aprotic solvents. Table 7 shows the results for non-polar aprotic solvents. Although a lot of time and effort was expended on these simulations, no trend which favors one polymorph or the other emerges for different solvent levels. Thus, the use of the periodic condition in MD simulations was not able to offer any new guidance, presumably due to the inability to calculate

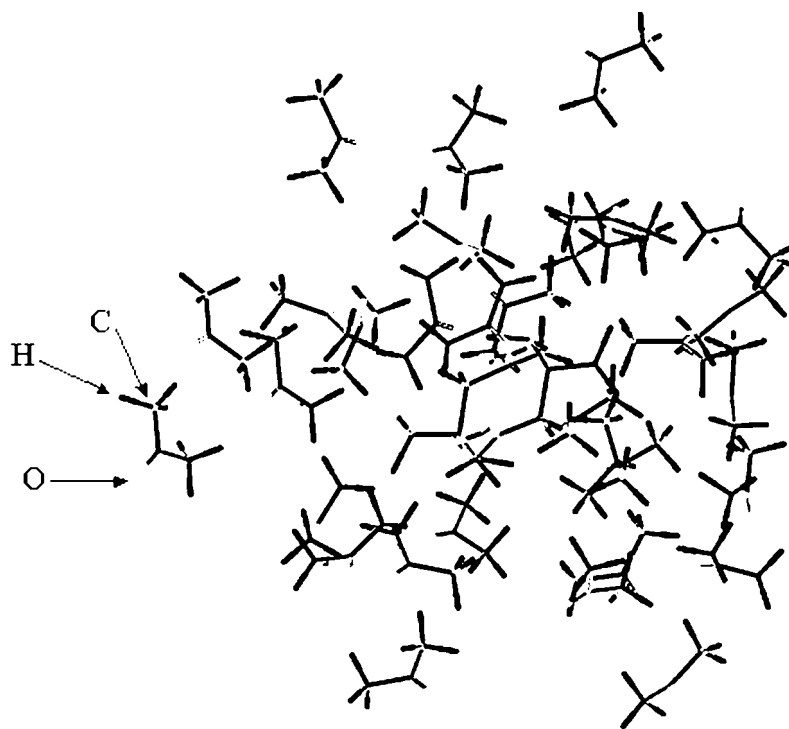


**Figure 8.** Non periodic boundary condition of HNFx with acetone.

and incorporate the contribution of the entropy term to the determination of the Gibbs free energy. The modeling results however, turned out to be very different for the CL-20 crystallization as outlined next.

*Mathematical Modeling Results for the Crystallization of CL-20.* CL-20 is a cage structure organic molecule with six nitro groups (Fig. 10a). In Fig 10b, the conformations of epsilon CL-20 molecules in the crystal lattice are demonstrated. Two of the nitro groups are open outwards in each epsilon CL-20 molecule. Gas phase MD simulation of CL-20 molecule at 300 K is performed under constant volume, constant energy condition in order to understand the vibrational motion of

**Table 4**  
Molecular dynamic simulation: Non-periodic conditions for HNFx, in the presence of solvents

*Solvents	HNFx, exp. R-3	Polymorphs				
		*Pca2 <sub>1</sub>	*P2 <sub>1</sub> /c	*Cc	*P2 <sub>1</sub> P2 <sub>1</sub> P2 <sub>1</sub>	
Acetone (CH <sub>3</sub> COCH <sub>3</sub> )	-335.921	-352.050	-347.237	-524.953	-340.866	
Acetophenone (C <sub>6</sub> H <sub>5</sub> COCH <sub>3</sub> )	-778.196	-703.556	-763.605	-752.275	-730.289	
Chloroform (CHCl <sub>3</sub> )	-386.539	-390.090	-370.679	-290.252	-421.723	
Cyclohexanone (C <sub>6</sub> H <sub>10</sub> O)	-787.848	-661.868	-726.342	-812.731	-705.417	
Dichloromethane (CH <sub>2</sub> Cl <sub>2</sub> )	-485.024	-473.349	-453.864	-446.314	-546.951	
Ethanol (C <sub>2</sub> H <sub>5</sub> OH)	-658.253	-781.180	-393.63	-612.732	-440.363	
Ethyl acetate (CH <sub>3</sub> COOC <sub>2</sub> H <sub>5</sub> )	-884.139	-855.010	-828.980	-861.798	-781.836	

\*32 molecules of solvent were used in each case.

nitro groups. The results show that the vibrational motion of four nitro groups in pentagon rings are relatively strong and the four stable polymorphs would involve different orientations of these nitro groups.

A typical realistic simulation of the recrystallization of CL-20, carried out by using a periodic boundary condition in which the simulated molecules within the cubic box replicate themselves in each direction is shown in Fig. 11. The antisolvent poly (dimethylsiloxane) was also incorporated into the simulation. The simulation box (CL-20 in 50% by mole EAC-PDMS) with a density of 0.9 g/cc is generated by using an amorphous builder module. The model is further minimized and then simulated by using nVE method for 10 ps. The results are saved as a trajectory file in each time step. The formation of stable phases of CL-20 is monitored based on conformational changes. The relative distribution of polymorphs after 10 ps is

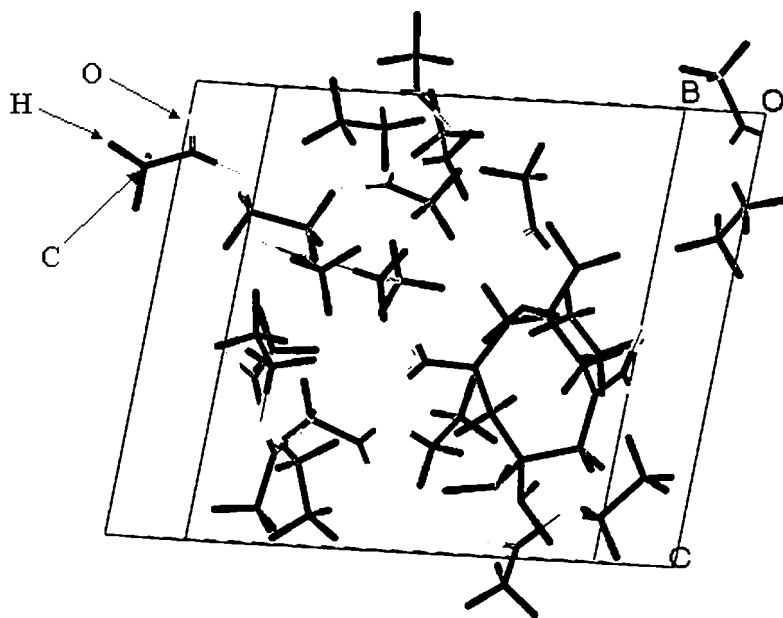


**Figure 9.** Periodic condition of HNFx with ETAC.

**Table 5**  
Molecular dynamic simulation: Periodic conditions in the presence of solvents

*Polar protic solvent	HNFX, exp. R-3	Polymorphs				
		*Pca2 <sub>1</sub>	*P2 <sub>1</sub> /c	*Cc	*P2 <sub>1</sub> P2 <sub>1</sub> P2 <sub>1</sub>	
Acetic acid (CH <sub>3</sub> COOH)	-940.409	-1007.12	-1208.49	-683.177	-523.205	
Benzyl alcohol (C <sub>6</sub> H <sub>5</sub> CH <sub>2</sub> OH)	-1305.77	-1831.76	-1705.98	-1631.17	-1234.04	
Ethanol (C <sub>2</sub> H <sub>5</sub> OH)	-681.026	-883.177	-1258.06	-737.057	-584.588	
Formic acid (HCOOH)	-937.822	-1002.44	-909.601	-1110.03	-817.606	
Formamide (NH <sub>2</sub> COH)	-1263.24	-1100.82	-1049.73	-1668.56	-990.710	
Methanol (CH <sub>3</sub> OH)	-1194.52	-1112.75	-809.359	-869.729	-1270.54	
Water (H <sub>2</sub> O)	-1313.10	-1627.74	-1500.04	-1508.46	-1235.10	

\*32 molecules of solvent were used in each case.

**Table 6**  
Molecular dynamic simulation: Periodic conditions in the presence of solvents

*Non-polar aprotic solvent	HNFX, exp. R-3	Polymorphs			
		*Pca2 <sub>1</sub>	*P2 <sub>1</sub> /c	*Cc	*P2 <sub>1</sub> P2 <sub>1</sub> P2 <sub>1</sub>
Benzene (C <sub>6</sub> H <sub>6</sub> )	-968.627	-803.795	-955.748	-1046.79	-834.284
Chloroform (CHCl <sub>3</sub> )	-507.243	-848.697	-567.559	-574.637	-629.382
Cyclohexane (C <sub>6</sub> H <sub>12</sub> )	-356.278	-446.385	-731.875	-718.535	-674.963
Dichloromethane (CH <sub>2</sub> Cl <sub>2</sub> )	-714.879	-665.205	-901.231	-787.988	-947.658
Heptane (C <sub>7</sub> H <sub>16</sub> )	-988.380	-1532.69	-1074.85	-1579.20	-1216.95
Hexane (C <sub>6</sub> H <sub>14</sub> )	-1149.33	-775.825	-869.142	-602.419	-1130.51
Toluene (C <sub>6</sub> H <sub>5</sub> CH <sub>3</sub> )	-966.675	-1017.11	-813.028	-940.468	-787.489

\*32 molecules of solvent were used in each case.

**Table 7**  
Molecular dynamic simulation: Periodic conditions in the presence of solvents

*Dipolar aprotic solvent	HNFX, exp. R-3	Polymorphs			
		*Pca2 <sub>1</sub>	*P2 <sub>1</sub> /c	*Cc	*P2 <sub>1</sub> P2 <sub>1</sub> P2 <sub>1</sub>
Acetone (CH <sub>3</sub> COCH <sub>3</sub> )	-667.489	-1478.43	-1108.44	-1075.09	-550.717
Acetonitrile (CH <sub>3</sub> CN)	-1297.36	-1854.24	-1369.27	-1051.08	-1306.78
Acetophenone (C <sub>6</sub> H <sub>5</sub> COCH <sub>3</sub> )	-1604.38	-1494.03	-1427.33	-1306.01	-1851.47
Cyclohexanone (C <sub>6</sub> H <sub>10</sub> O)	-1371.84	-1156.96	-1220.43	-1771.12	-1156.19
Dimethyl sulfoxide (CH <sub>3</sub> SOCH <sub>3</sub> )	-866.664	-828.034	-1042.25	-893.918	-1100.45
Dimethyl formamide (HCON(CH <sub>3</sub> )) <sub>2</sub>	-1354.23	-1285.25	-1685.63	-1929.90	-1620.50
Ethyl acetate (CH <sub>3</sub> COOC <sub>2</sub> H <sub>5</sub> )	-1592.61	-1491.51	-1942.32	-1063.71	-1881.46
1,4-dioxane (C <sub>4</sub> H <sub>8</sub> O <sub>2</sub> )	-694.804	-590.128	-819.285	-600.500	-865.446
Tetrahydropyran (C <sub>5</sub> H <sub>10</sub> O)	-825.755	-799.025	-804.750	-839.550	-889.507

\*32 molecules of solvent were used in each case.

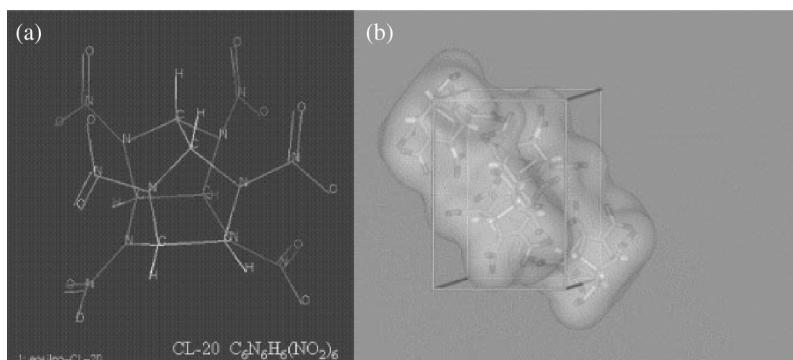


**Figure 10.** a) Molecular structure and b) unit cell structure of  $\epsilon$ -CL-20.

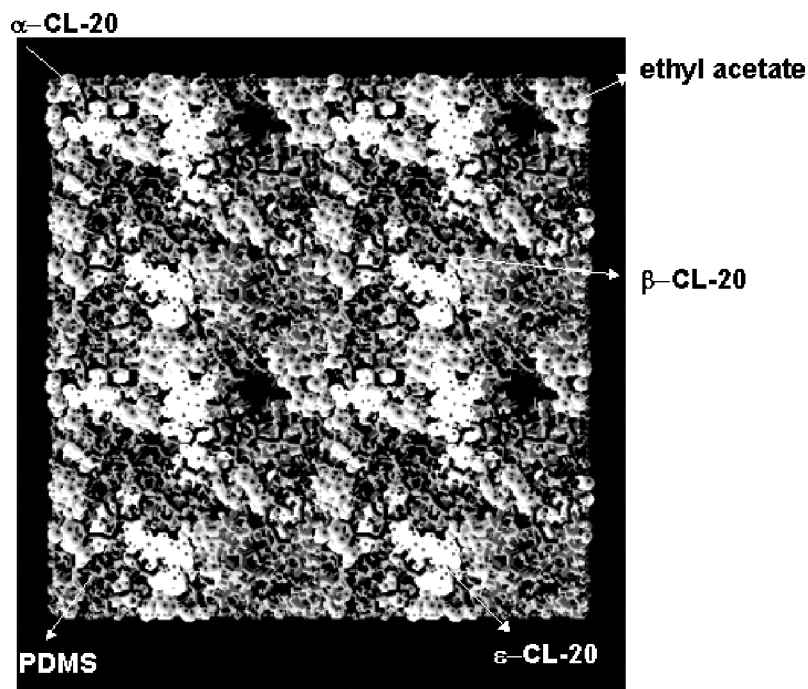


**Figure 11.** Molecular dynamics of CL-20 in 50% ethyl acetate-PDMS at  $t = 10$  ps which shows preferential formation of epsilon phase.

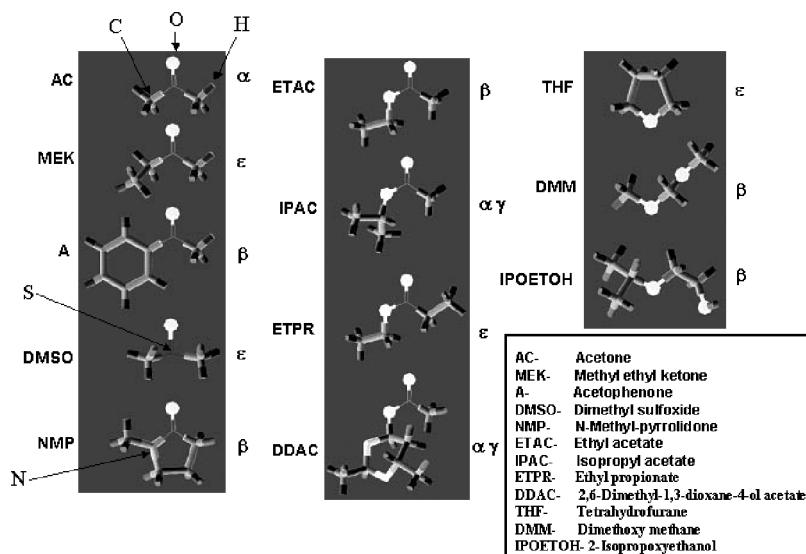


**Figure 12.** Predicted polymorph types of CL-20 for various solvent molecules.

seen in Fig. 11. Here we assume that the molecules maintain their stable conformations in solution during the nucleation of CL-20. The results show that the numbers of different polymorphs in the system are epsilon-(6) , alpha-(1) and beta-(1). Thus, it is predicted that the probability of formation of epsilon phase is 75% (6/8) in this solvent system. Thus, a mixture of polymorphs are predicted.

The results of our predictions of the different polymorph types to be generated upon using various solvents are summarized in Fig. 12. These results indicate that different polymorphs or combinations of different polymorphs of CL-20 are likely. As Part II of this paper will show these predictions turn out to be quite accurate in predicting that multiple polymorphs will be generated. In Part II first the development of experimental means necessary for the determination of multiple polymorphs will be reported followed by data which indicate that multiple polymorphs indeed form upon recrystallization of CL-20.

## Conclusions

Various mathematical models were used for the determination of the type of polymorph to be generated when different crystallization conditions/solvents are used during the recrystallization of CL-20 and HNFx. The results indicated that different polymorphs or combinations of polymorphs are likely to emerge upon the recrystallization of CL-20 and HNFx. As will be shown in Part II of this paper (same issue) although multiple polymorphs were indeed observed upon the recrystallization of CL-20 from different solvents, only one polymorph was observed for HNFx, i.e., the Ci R-3 polymorph.

## Acknowledgements

We wish to express our gratitude to Dr. Judah Goldwasser and the Office of Naval Research for the financial support for this project under grant # N00014-03-1-0775 and to Dr. James Baldwin and his colleagues at China Lake for the HNFx used in the experiments and for their generous help and input on various facets of the project. We also express our gratitude to Picatinny ARDEC for the funding of the CL-20 crystallization study under contract DAAE30-00-D-1011-Task #1 and thank T. McWilliams, A. Perich, D. Fair, M. Mezger, K. Jasinkiewicz, E. Begasse, P. Redner and D. Gilson of ARDEC for their help and input. We also thank Dr. B. Greenberg and Dr. S. Koven of Stevens for their contributions and suggestions.

## References

- [1] Pagoria, P. F., G. S. Lee, A. R. Mitchell, and R. D. Schmidt. 2002. A review of energetic materials synthesis. *Thermochimica Acta.*, 384: 187–204.
- [2] Christe, K., W. Wilson, M. Petrie, H. Michels, J. Bottaro, and R. Gilardi. 1996. The dinitramide anion. *Inorg. Chem.*, 35: 5068–5071.
- [3] Shevelev, S. A., I. L. Dalinger, T. K. Shkineva, B. I. Ugrak, V. I. Gulevskaya, and M. I. Kanishchev. 1993. Nitropyrazoles, Synthesis, transformations, and physicochemical properties of

- nitro derivatives of 1H, 4H-pyrazolo[4,3-c] pyrazole. *Russian Chemical Bulletin*, 42, 6: 1063–1068.
- [4] Litvinov, V., A. A. Fainzil'berg, V. I. Pepekin, S. P. Smirnov, B. G. Lobiko, S. A. Shevelev, and G. M. Nazin. 1994. *DokLady Chemistry*, 336: 1–3.
- [5] Chapman, R. D., R. D. Gilardi, M. F. Welker, and C. B. Kreutzberger. 1999. Nitrolysis of a highly deactivated amide by protonitronium. Synthesis and structure of HNFx. *J. Org. Chem.*, 64: 960.
- [6] Kamlet, M. J. and S. J. Jacobs. 1968. Chemistry of detonations. I. A simple method for calculating detonation properties of C–H–N–O explosives. *J. Chem. Phys.*, 48: 23–36.
- [7] Ammon, J. H. L., R. Holden, and Z. Du. 2002. Structure and Density Predictions for Energetic Materials. Energetic Materials Design for Improved Performance-Low Life Cycle Cost Kick-off Meeting, Aberdeen Proving Ground, MD.
- [8] von Holtz, E., D. Ornellas, M. F. Foltz, and J. E. Clarkson. 1994. The solubility of  $\epsilon$ -CL-20 in selected materials. *Propellants, Explosives, Pyrotechnics*, 19: 206–212.
- [9] Vippagunta, S. R., H. G. Brittain, and D. J. W. Grant. 2001. Crystalline solids, *Adv. Drug Delivery Reviews*, 48: 3–26.
- [10] Payne, R. S., R. J. Roberts, R. C. Rowe, R. Docherty. 1999. *International Journal of Pharmaceutics*, 177: 231–245.
- [11] Motherwell, W. D., H. L. Ammon, J. D. Dunitz, A. Dzyabchenko, P. Erk, A. Gavezzotti, D. W. M. Hofmann, F. J. Leusen, J. P. Lommerse, W. T. Mooij, S. L. Price, H. Scheraga, B. Schweizer, M. U. Schmidt, B. P. van Eijck, P. Verwer, and D. E. Williams. 2002. Crystal structure prediction of small organic molecules: a second blind test. *Acta Cryst.*, B58: 647–661.
- [12] Lommerse, J. P. M., W. D. S. Motherwell, H. L. Ammon, J. D. Dunitz, A. Gavezzotti, D. W. M. Hofmann, F. J. J. Leusen, W. T. M. Mooij, S. L. Price, B. Schweizer, M. U. Schmidt, B. P. van Eijck, P. Verwer, and D. E. Williams. 2000. A test of crystal structure prediction of small organic molecules. *Acta Cryst.*, B56: 697–714
- [13] Cerius2, September 1988. *Analytical Instruments*. San Diego: Molecular Simulations Inc.
- [14] Leusen, F. J. J., S. Wilke, P. Werner, and G. E. Engel. 1999. Computational approaches to crystal structure and polymorph prediction. In J. A. K. Howard, F. H. Allen, and G. P. Shields, (eds.), *Implications of Molecular and Materials Structure for*

- New Technologies, NATO, Science series. E. Dordrecht, The Netherlands: Kluwer Academic, vol. 360, 303–314.*
- [15] Kendrick, J., E. Robson, W. Leeming, G. A. Leiper, A. S. Cumming, and C. Leach. 1997. Waste management. *Molecular Modeling of Novel Energetic Materials*, 17, 2–3: 187–189.
- [16] Givand, J., P. J. Ludovice, R. W. Rousseau. 1998. Characterization of L-isoleucine crystal morphology from molecular modeling. *J. Cryst. Growth.*, 194: 228–238.
- [17] Mayo, S. L., B. D. Olafson, and W. W. Goddard. 1990. DREIDING: a generic force field. *J. Phys. Chem.*, 94: 8897–8909.
- [18] Bunte, S. W. and H. Sun. 2000. Molecular modeling of energetic materials: The parameterization and validation of nitrate esters in the COMPASS force field. *J. Phys. Chem. B.*, 104, 11: 2477–2489.
- [19] Aabloo, A., M. Klintonberg, and J. O. Thomas. 2000. Molecular dynamics simulation of a polymer-inorganic interface. *Electrochimica Acta.*, 45: 1425–1429.
- [20] Nagarajan, K. and A. S. Myerson. 2001. Molecular dynamics of nucleation and crystallization of polymers. *Crystal Growth and Design*, 1, 2: 131–142.